THERMODYNAMIC PROPERTIES OF UNDERDOPED $YBa_2Cu_3O_{6+x}$ CUPRATES FOR SEVERAL DOPING VALUES

P. SALAS [*], M. A. SOLIS, M. FORTES and F. J. SEVILLA

*Instituto de Física, Universidad Nacional Autónoma de México,
Apdo. Postal 20-364, 01000 Ciudad de México, México*

patysalasc@fisica.unam.mx

We report the thermodynamic properties of cuprate superconductors $YBa_2Cu_3O_{6+x}$, with x ranging from underdoped (x = 0.55) to optimally doped (x = 0.9) regions. We model cuprates as a boson-fermion gas mixture immersed in a layered structure, which is generated via a Dirac comb potential applied in the perpendicular direction to the CuO_2 planes, while the particles move freely in the other two directions. The optimal system parameters, namely, the planes' impenetrability and the paired-fermion fraction are obtained by minimizing the Helmholtz free energy in addition to fixing the critical temperature T_c to its experimental value. Using this optimized scheme, we calculate the entropy, the Helmholtz free energy and the specific heat as functions of temperature. Additionally, some fundamental properties of the electronic specific heat are obtained, such as the normal linear coefficient $\gamma(T_c)$, the quadratic α term and the jump height at T_c. We reproduce the cubic β_l term of the total specific heat for low temperatures. Also our multilayer model inherently brings with it the mass anisotropy observed in cuprate superconductors. Furthermore, we establish the doping value beyond which superconductivity is suppressed.

Keywords: Underdoped cuprates; Superconductivity; Helmholtz free energy; Specific heat.

1. Introduction

A great amount of theoretical work has been invested in pursuing a better description of the properties of the High Temperature Superconductors (HTSC) since their discovery[1], in an effort to go beyond the models provided by the BCS theory[2]. Most of these models are BCS-*type* theories, and very few of them extend their predictions to the thermodynamic properties other than the critical temperature, such as the Helmholtz free energy or the specific heat. In addition, the influence of doping is hardly ever mentioned in theoretical calculations, even though there is abundant experimental material that can be found in the literature.

Most recent investigations focus on the newer kinds of superconductors such as FeAs[3,4] and H_2S[5,6], which has the record of highest T_c. Therefore it is not surprising

---

[*]Correspondig author.

that experiments that report advances on cuprates frequently go unnoticed. However, these advances have lead us to a deeper understanding of the relation among their properties and the superconducting state. Some of them are: the notorious increase in the value of the superconducting gap for underdoped cuprates as doping diminishes[7]; the dramatic decrease of the Fermi temperature with doping[8]; the dependence of hole concentration *vs* oxygen content[9], and the dependence of doping on the cell size[10], among others.

In this work, we use the Boson-Fermion model of superconductivity[11,12,13,27,30] and its recently developed extension to layered systems[26] to study the influence of doping on the thermodynamic properties of underdoped cuprates $YBa_2Cu_3O_{6+x}$, with $x \in [0.55, 0.9]$. To model the cuprate superconductors, we begin with an electron gas subject to a BCS interaction and immersed in a multilayer structure which represents the CuO_2 planes. As the temperature is lowered, the electron pairing starts at some temperature T^*, while coherence among the Cooper pairs is reached a the critical temperature $T_c < T^{*}$[13,14,15,16]. At this stage, the Cooper pairs behave like composite, non-interacting spin-zero bosons[17], with either zero or nonzero center-of-mass momenta, coexisting with the fermion fluid of unpaired electrons immersed in a periodic multilayer array[18,19,20] in a ratio that depends on the characteristics of each superconductor. Whether the temperature T^* represents the pseudogap temperature as a sign of pre-pairing[7,21,22,23] or not[24,25] is still an ongoing debate.

The paper is organized as follows: in Sec. 2 we describe the Boson-Fermion Layered model where we derive the bosonic and fermionic thermodynamic grand potentials. The multilayer array is generated by an external Kronig-Penney (KP) potential at the delta limit (Dirac-comb potential) along the perpendicular direction to the CuO_2 planes, while the particles are allowed to move freely in the plane parallel directions[26]. In Sec. 3 we calculate the critical temperature for several underdoped cuprates in terms of our system parameters P_0 and f, which are the plane impenetrability and the fraction of pairable fermions, respectively. Upon minimization of the Helmholtz free energy we optimize these parameters, and, together with the phonon contribution from the the lattice spectrum reported by ARPES, as in Ref. 23 , we obtain the thermodynamic properties as functions of temperature for several doping values. We also present our results for the specific heat constants and the mass anisotropy *vs* doping. Conclusions and final remarks are presented in Sec. 4.

2. The Model

We start with a system of N electrons of mass m_e interacting via a BCS-type potential immersed in a periodic layered array. It is assumed that there is a set of *pairable* electrons in momentum space within a shell of width $2\hbar\omega_D$ around the Fermi energy E_F, where $\hbar\omega_D$ is the Debye energy of the superconductor. This set coexists with a group of non-pairable electrons, namely those outside the pairing shell which are not eligible for pairing. In the first set, we assume that only a small fraction

$(fN/2)$ of them are *paired* at $T = T_c$, and which participate in the superconduction. This assumption, also valid for underdoped cuprates[27], is based on the analysis made in Ref. 26 of Uemura's plot[28,29], in which the Fermi energy is represented as a function of the superconducting particle density. Thus, the N electrons are grouped in three major components: paired electrons (boson gas) formed by a fraction f of half the total N electrons; a fermion gas of the pairable but unpaired electrons (also inside the pairing shell); and the unpairable electrons (outside the pairing shell). We assume that the number of pairs at T_c remains constant as temperature is lowered, although it could increase by a mechanism not yet considered in this model.

The composite bosons of mass $m = 2m_e$ are Cooper pairs that appear as resonances in two electrons or two holes, as proposed by Friedberg and Lee[11,12]. The corresponding Hamiltonian is

$$H = \sum_{\mathbf{k},s} \varepsilon_{\mathbf{k}} a_{\mathbf{k},s}^{\dagger} a_{\mathbf{k},s} + \sum_{\mathbf{K}} \varepsilon_{\mathbf{K}} b_{\mathbf{K}}^{\dagger} b_{\mathbf{K}} + H_1, \tag{1}$$

where $a_{\mathbf{k},s}^{\dagger}$ $(a_{\mathbf{k},s})$ and $b_{\mathbf{K}}^{\dagger}$ $(b_{\mathbf{K}})$ are fermion and composite-boson creation (annihilation) operators, respectively, s is the spin and

$$H_1 = \frac{\mathsf{G}}{\sqrt{L^3}} [a_{\mathbf{K}/2+\mathbf{k},s} a_{\mathbf{K}/2-\mathbf{k},s} b_{\mathbf{K}}^{\dagger} v(k) + h.c.] \tag{2}$$

is the interaction Hamiltonian that creates (destroys) composite bosons from (into) two fermions, where the wave vector for the center-of-mass momentum (CMM) of the pair is given by $\mathbf{K} = (K_x, K_y, K_z) \equiv \mathbf{k}_1 + \mathbf{k}_2$ with $\mathbf{k}_1$ and $\mathbf{k}_2$ the wave-vectors of each electron in the pair. The form factor $v(k)$ is normalized such that $v(0) = 1$, which defines the coupling constant G. The energy for each boson particle can be separated in the $x-y-$ and $z-$ directions as $\varepsilon_K = \varepsilon_{K_{x,y}} + \varepsilon_{K_z}$.

It has been shown[27,30] that when $|\mathbf{K}|$ is non zero but small, one can expand the binding energy from the Cooper equation in a series of powers with the linear term predominating, so that the total energy in the plane is

$$\varepsilon_{K_{x,y}} = \mathsf{e}_0 + C_1(K_x^2 + K_y^2)^{1/2}, \tag{3}$$

where $\mathsf{e}_0 \equiv 2E_F - \Delta_0$ is a constant, $C_1 = (2/\pi)\hbar \mathsf{v}_{F2D}$ is the linear term coefficient in 2D, v_{F2D} is the two-dimensional Fermi velocity, $\Delta_0 = 2\hbar\omega_D \exp(-1/\lambda)$ is the energy gap for $\mathbf{K} = 0$ in the weak-coupling regime (corresponding to the BCS theory), and λ is the electron-phonon coupling constant given by $\lambda = g(E_F)V$, with $g(E_F)$ the density of states at the Fermi energy and V the BCS interaction strength.

Along the z-direction we model the layers using the Dirac-comb potential, where the energies are implicitly obtained as a function of the separation between barriers a, from the transcendental equation[18,19]

$$[P_0(a/\lambda_0)\sin(\alpha_{K_z}a)]/(\alpha_{K_z}a) + \cos(\alpha_{K_z}a) = \cos(K_z a), \tag{4}$$

4   *P. Salas et al.*

with $\alpha_{K_z}^2 \equiv 2m\varepsilon_{K_z}/\hbar^2$, and $P_0 = m\Lambda\lambda_0/\hbar^2$ is a measure of the plane impenetrability. The constant $\lambda_0 \equiv h/\sqrt{2\pi mk_BT_0}$ is the de Broglie thermal wavelength of an ideal boson gas in an infinite box at the BEC critical temperature $T_0 = 2\pi\hbar^2 n_B^{2/3}/mk_B\zeta(3/2)^{2/3} \simeq 3.31\hbar^2 n_B^{2/3}/mk_B$, with $n_B \equiv N/(2L^3)$ the boson number density and Λ the strength of the KP delta potentials $\sum_{n_z=-\infty}^{\infty} \Lambda\delta(z-n_z a)$. In what follows, the plane separation a will be taken as half the crystallographic constant c of the cuprates, considering that there are two copper-oxide regions per unit cell where superconductivity takes place.

The non-paired fermions are subject to the same external KP potential Eq. (4) in $z-$direction and they move freely in the $x - y$ directions[20], with their single particle energies given by $\varepsilon_k = \varepsilon_{k_x} + \varepsilon_{k_y} + \varepsilon_{k_z}$.

We first obtain the grand potential for each component to calculate the corresponding thermodynamic properties. Hence, for the boson gas we have

$$\Omega_B\left(T, L^3, \mu_B\right) = k_BT \ln\left\{1 - \exp[-\beta(\varepsilon_0 + \mathsf{e}_0 - \mu_B)]\right\} -$$
$$\frac{1}{\beta^3}\frac{L^3}{(2\pi)^2}\frac{\Gamma(2)}{C_1^2}\int_{-\infty}^{\infty} dK_z \; \mathsf{g}_3\left\{\exp[-\beta(\varepsilon_{K_z} + \mathsf{e}_0 - \mu_B)]\right\}, \tag{5}$$

where μ_B is the boson chemical potential, $\beta \equiv 1/k_BT$, $\varepsilon_0 \equiv \hbar^2\alpha_0^2/2m$ the solution of Eq. (4) for the ground state energy, and $\mathsf{g}_\sigma(t) \equiv \sum_{l=1}^{\infty}(t)^l/l^\sigma$ are the Bose functions [31]; while for the unpaired fermions we have

$$\Omega_F\left(T, L^3, \mu_F\right) = -2\frac{L^3}{(2\pi)^2}\frac{m_e}{\hbar^2}\frac{1}{\beta^2}\int_{-\infty}^{\infty} dk_z \; \mathsf{f}_2\left\{\exp[-\beta(\varepsilon_{k_z} - \mu_F)]\right\}, \tag{6}$$

where μ_F is the chemical potential of the fermions, $\varepsilon_k = \hbar^2 k_x^2/2m_e + \hbar^2 k_y^2/2m_e + \varepsilon_{k_z}$ is their energy, $\mathsf{f}_\sigma(t) \equiv -\sum_{l=1}^{\infty}(-t)^l/l^\sigma$ are the Fermi-Dirac functions, and where the spin degeneracy has already been taken into account.

3. Thermodynamic properties

We calculate the thermodynamic properties using the grand potential (5) for the Cooper pairs and (6) for the normal state fermions.

3.1. *Critical temperature*

We assume that the superconducting critical temperature is the BEC temperature of the pairs obtained from the boson number equation derived directly from Eq. (5),

$$N_B = \frac{1}{\exp\left\{\beta(\varepsilon_0 + \mathsf{e}_0 - \mu_B)\right\} - 1} + \frac{L^3}{(2\pi)^2}\frac{\Gamma(2)}{C_1^2}\frac{1}{\beta^2}$$
$$\times \int_{-\infty}^{\infty} dK_z \mathsf{g}_2\left\{\exp[-\beta(\varepsilon_{K_z} + \mathsf{e}_0 - \mu_B)]\right\}, \tag{7}$$
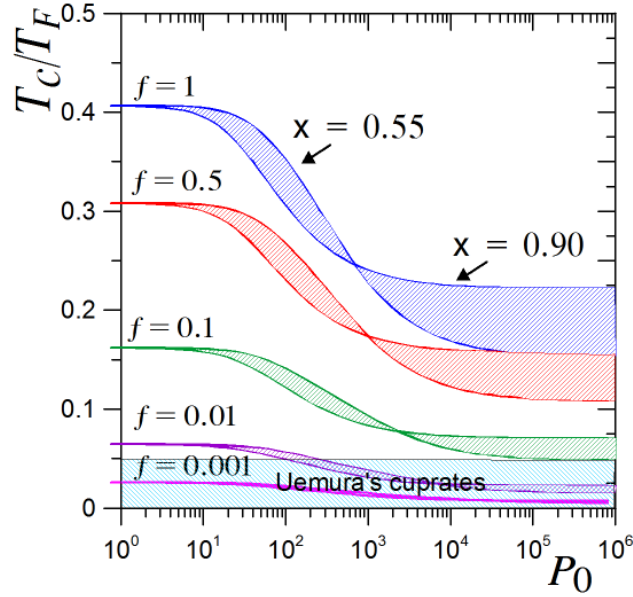
Fig. 1.   (Color online) Critical temperature, computed from Eq. (8) in units of the doping-dependent Fermi temperature *vs* the impenetrability P_0 for different values of paired electrons f (in color) and for values of the doping x between 0.55 and 0.9.

where in the rhs we have separated the number of particles in the condensate $N_{B0}(T)$ from those in the excited state (first and second term, respectively). At $T = T_c$ we introduce the conditions $\mu_0 = \varepsilon_0 + \mathsf{e}_0$ and $N_{B0}(T_c)/N_B \simeq 0$, so

$$N_B = \frac{L^3}{(2\pi)^2} \frac{\Gamma(2)}{C_1^2} \frac{1}{\beta_c^2} \int_{-\infty}^{\infty} dK_z \mathsf{g}_2 \big\{ \exp[-\beta_c(\varepsilon_{K_z} - \varepsilon_0)] \big\}, \tag{8}$$

where $\beta_c \equiv 1/k_B T_c$.

Introducing the values for the superconducting gap Δ_0[7], the Fermi temperatures[8] and the cell size[10] reported in the literature for the cuprates YBa$_2$Cu$_3$O$_{6+x}$, with x varying from underdoped (x = 0.55) to optimally doped (x = 0.90), we calculate the critical temperature of each cuprate as a function of P_0 for several values of f, as shown in Fig. 1. The shaded areas are the allowed values for the parameters P_0 and f, limited by the critical temperatures of the extreme doping values x = 0.55 and 0.90, respectively. This procedure indicates that the fraction f must be under $1 - 2\%$, which is consistent with Ref. 23 , if the experi-

mental critical temperatures (as shown in Uemura's plot[28]) are to be reproduced. However, the exact values of our system parameters P_0 and f have to be determined by other methods, as will be done in the next section by minimizing the Helmholtz free energy. Furthermore, this procedure loses consistency for doping values below $x = 0.55$, which is in agreement with the suppression of superconductivity at approx. $x = 0.5$ reported in Ref. 8.
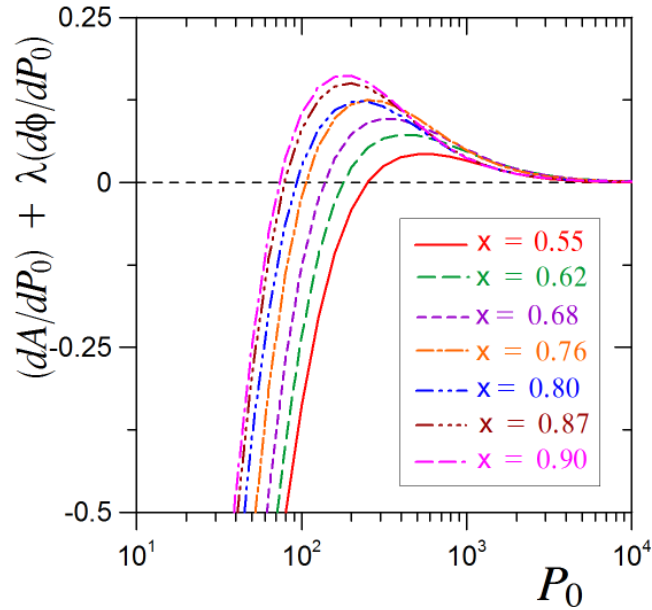
Fig. 2.   (Color online) Minimization of the total electronic Helmholtz free energy for several doping values.

3.2. *Electronic Helmholtz free energy*

The optimal values for (P_0, f) are obtained by minimizing the total electronic Helmholtz free energy A that includes the Cooper pairs component (superconducting) and the free fermion (normal) component, $A = A_{es} + A_{en}$. We fix the critical temperature to the experimental value, *i.e.* $T_c = T_{c-exp}$, in the Boson-Number Eq. (8) and use it as the condition in the Lagrange multipliers' method. In Fig. 2 we plot this condition, namely, the derivative of the Helmholtz free energy together
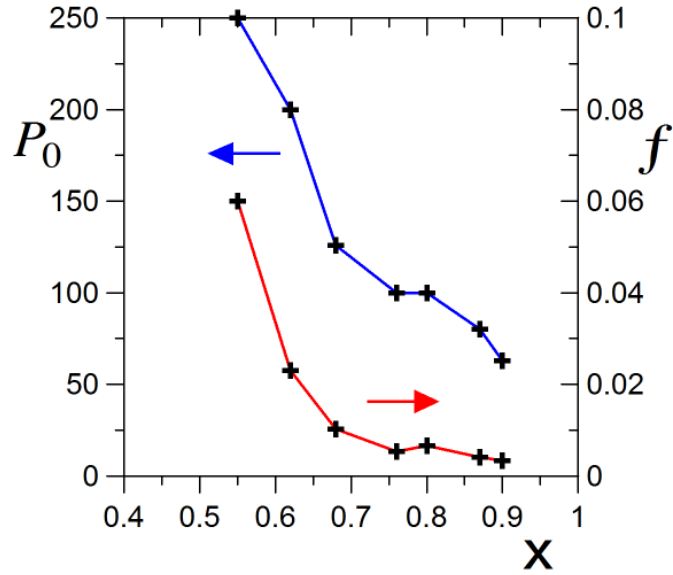
Fig. 3.   (Color online) Optimal parameters P_0 and f, for each doping value x.

with the constraint. The roots provide the optimal parameters values (P_0, f) for each doping value x, which are shown in Fig. 3.

3.3. *Electronic entropy*

Once the parameters of the model have been set for each doping value, we may obtain the thermodynamic properties as functions of temperature. This is shown in Fig. 4, where the calculated electronic entropy $S_e = S_{es} + S_{en}$ is plotted together with a curve obtained from the experimental electronic specific heat reported in Fig. 5 of Ref. 23 for a doping value x = 0.7, which we compare with our results for x = 0.68. We are aware that the curvature of the experimental result below 40 K is lower than ours, and we attribute this to the fact that we are not allowing the pair formation at temperatures below the critical temperature. Also, there are other possible disorder sources not considered in our model, such as the suppression of the spin susceptibility[32] and oxygen disorder[33].

8   *P. Salas et al.*
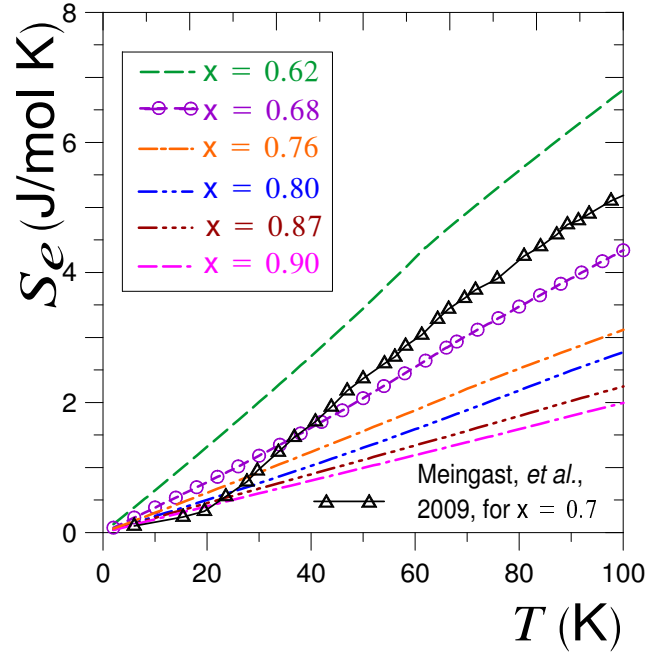
Fig. 4.   (Color online) Electronic entropy for several doping values x. The line with open triangles is the calculated entropy obtained from the electronic specific heat of Ref.23, to be compared with the line with open circles from the present work.

3.4. *Specific heat*

The total constant-pressure specific heat is $C_p = C_{pes} + C_{pen} + C_l$, where the boson gas component C_{pes} is given by

$$
\frac{C_{pes}}{N_B k_B} = \frac{C_{Ves}}{N_B k_B} - \left(\frac{\int_{-\infty}^{\infty} dK_z \ln\{1 - \exp[-\beta(\varepsilon_{K_z} + \mathsf{e}_0 - \mu_B)]\}}{\int_{-\infty}^{\infty} dK_z \mathsf{g}_2\{\exp[-\beta(\varepsilon_{K_z} + \mathsf{e}_0 - \mu_B)]\}} \right)
$$
$$
\times \left(\frac{L^3}{(2\pi)^2} \frac{\Gamma(2)}{C_1^2} \frac{1}{\beta^2} \left[3 \int_{-\infty}^{\infty} dK_z \mathsf{g}_3\{\exp[-\beta(\varepsilon_{K_z} + \mathsf{e}_0 - \mu_B)]\} \right.\right.
$$
$$
\left.\left. + \beta \int_{-\infty}^{\infty} dK_z \mathsf{g}_2\{\exp[-\beta(\varepsilon_{K_z} + \mathsf{e}_0 - \mu_B)]\} \right] \right)^2 , \qquad (9)
$$
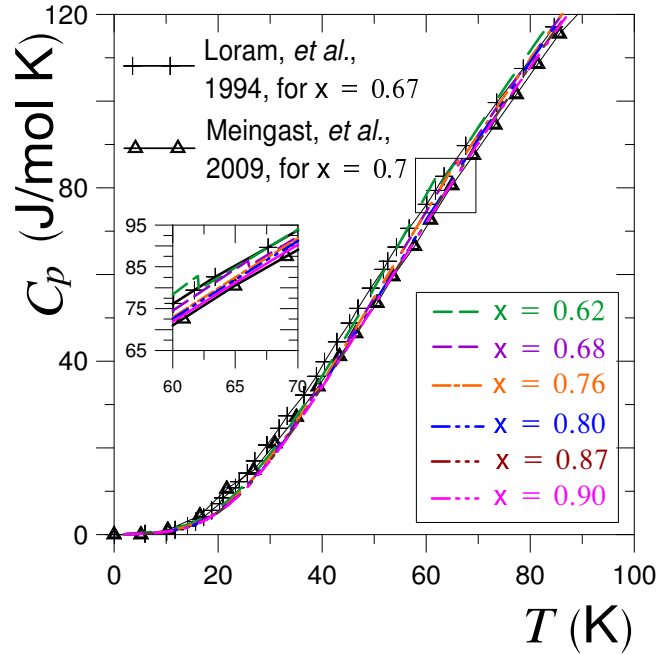
Fig. 5.   (Color online) Total constant pressure specific heat as function of temperature for several doping values ranging from x = 0.62 to 0.90. *Inset: close view of the transition zone.*

where C_{Ves} is the constant volume specific heat for the bosons. The corresponding fermion component C_{pen} is given by

$$\frac{C_{pen}}{Nk_B} = \frac{C_{Ven}}{Nk_B} + \frac{2L^3}{(1-f)N(2\pi)^2}\frac{m_e}{\hbar^2}\beta\left(\frac{\int_{-\infty}^{\infty}\frac{dk_z}{\exp[\beta(\varepsilon_{k_z}-\mu_F)]+1}}{(\int_{-\infty}^{\infty}dk_z\ln\{1+\exp[-\beta(\varepsilon_{k_z}-\mu_F)]\})^2}\right)$$

$$\times\left(\int_{-\infty}^{\infty}dk_z\ln\{1+\exp[-\beta(\varepsilon_{k_z}-\mu_F)]\}\left[\varepsilon_{k_z}-\mu_F+T\frac{d\mu_F}{dT}\right]\right.$$

$$\left.+\frac{2}{\beta}\int_{-\infty}^{\infty}dk_z\mathsf{f}_2\{\exp[-\beta(\varepsilon_{k_z}-\mu_F)]\}\right)^2 (10)$$

The phonon specific heat C_l is obtained in Ref. 26 from ARPES, which represents the major contribution to the total C_p, as shown in Figs. 5 and 6 for several doping values, together with the curves taken from the "raw data" of two different experiments[23,34]. Although we use C_l for the YBa$_2$Cu$_3$O$_7$ cuprate in every curve, it has been shown[26] that the variation in the phonon density of states due to doping
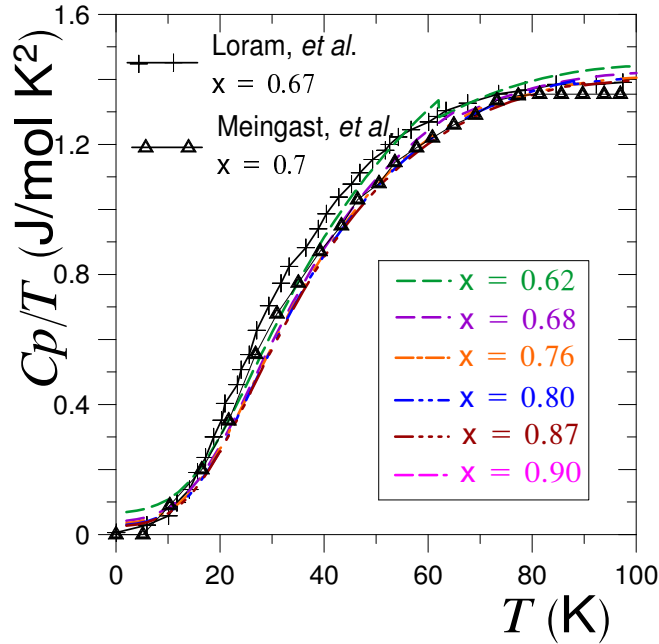
Fig. 6.   (Color online) Total constant pressure specific heat over temperature as functions of temperature for several doping values ranging from x = 0.62 to 0.90.

is very small and is not significant for the final result.

3.5.   *Specific heat constants and jump height as functions of doping*

Our results for the specific heat constants $\gamma_n(T_c) = C_p/T_c$, α (quadratic term coefficient) and β_l (cubic term coefficient for low temperatures) as functions of doping are presented in Figs. 7 and 8, together with the jump height $\Delta C_p/T_c$. To compare, we added some experimental data, which show a random behavior in the sense that most authors usually present only one point, mostly in the overdoped region, however, they all lie in the same order of magnitude. In Fig. 7 the experimental values for α are shown with filled symbols and open symbols for β_l, while in Fig. 8 we use filled symbols for $\Delta C_p/T_c$ and open ones for $\gamma_n(T_c)$. In particular, there is a series of values obtained by Wright *et al.*[35] and Moler *et al.*[36,37], which we show in Fig. 7, where the data show the same tendency as our results.

Whereas there are experimental data values for γ versus doping at temperatures
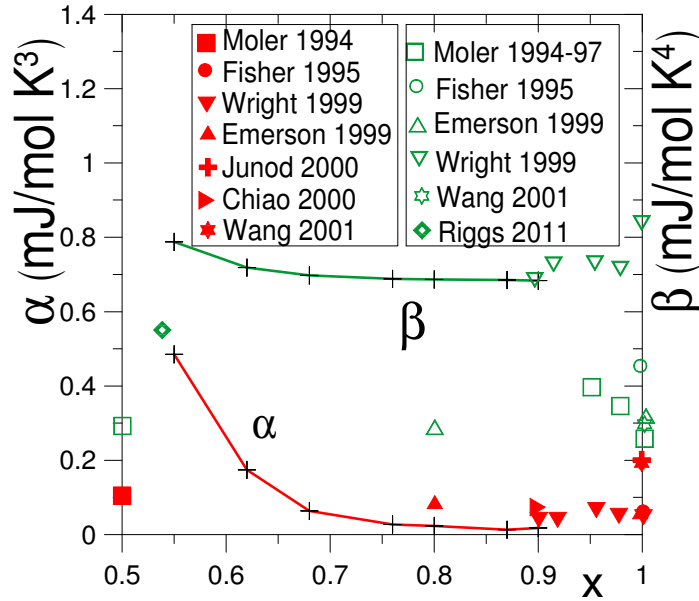
Fig. 7. (Color online) Quadratic α and cubic β specific heat coefficients as functions of doping. Filled symbols are for α experimental data and open symbols are for β_l data. Data is taken from Refs.: Riggs 2011 [33], Wright 1999 [35], Moler 1994-97 [36,37] , Fisher 1995 [38], Emerson 1999 [39], Junod 2000 [40], Chiao 2000 [41] and Wang 2001 [42].

near zero, these are absent at T_c. However, extrapolations to the overdoped side, as shown in Fig. 8, do lie in the correct order of magnitude. Furthermore, our calculations produce results of the correct order of magnitude for the jump height $\Delta C_p/T_c$. We note, however, that our curve shows a decreasing tendency in contrast with the rising trend shown in experiments, which is an indirect confirmation that additional effects compete with the layered structure model at temperatures near and equal to T_c.

3.6. *Mass anisotropy as a function of doping*

The mass anisotropy we present here is a direct connection between a physical observable of the cuprates and our model parameters, in the absence of external magnetic fields, and represents an alternative way to the mass tensor derivation from the Ginzburg-Landau equations[45]. We start by expanding the first term of the

12   *P. Salas et al.*
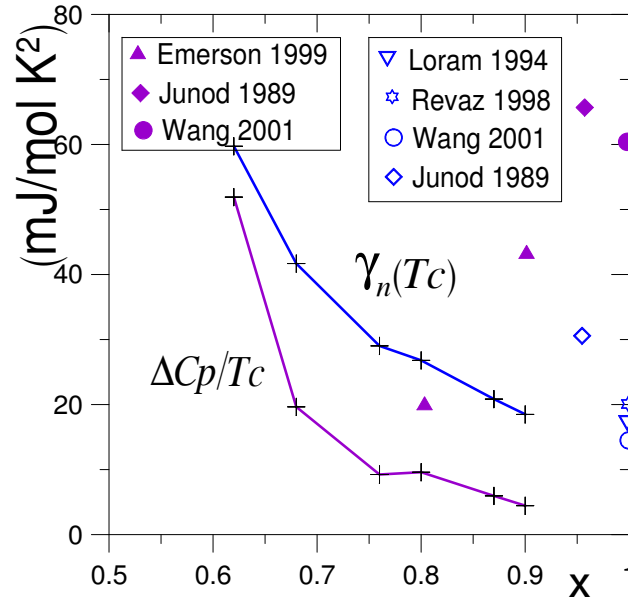
Fig. 8.   (Color online) Linear $\gamma_n(T_c)$ specific heat term at T_c and jump height $\Delta C_p/T_c$ as functions of doping. Filled symbols are for $\Delta C_p/T_c$ experimental data and open symbols are for $\gamma_n(T_c)$ data. Data is taken from Refs.: Loram 1994 [34], Emerson 1999 [39], Wang 2001 [42], Junod 1989 [43] and Revaz 1998 [44].

dispersion relation (4) for small particle energies $\varepsilon_{K_z} << \hbar^2/2ma^2$ around ε_0

$$\varepsilon_{K_z} \cong \varepsilon_0 + \frac{\hbar^2}{Ma^2}(1 - \cos K_z a), \tag{11}$$

where ε_0 is the solution to Eq. 4 when $K_z = 0$, namely,

$$P_0(a/\lambda_0)\sin(\alpha_0 a)/\alpha_0 a + \cos(\alpha_0 a) = 1, \tag{12}$$

and M is the effective mass in the z-direction. Solving for M/m one obtains

$$M/m = |[\sin(\alpha_0 a) - (P_0(a/\lambda_0) + 1)\cos(\alpha_0 a)/(\alpha_0 a)]/(\alpha_0 a)|. \tag{13}$$

Table 1.   Mass anisotropy as a function of doping YBa$_2$Cu$_3$O$_{6+x}$.

$6 + x$	6.55	6.62	6.68	6.76	6.8	6.87	6.9
M/m	3.75	3.69	2.89	2.76	2.9	2.62	2.25

Our results for the mass anisotropy of the $YBa_2Cu_3O_{6+x}$ cuprate are given in Table 1, which are of the same order of magnitude as those obtained from the series of experiments made by Roulin *et al.*[46] and Junod *et al.*[14]. Although our values are smaller than theirs, they show the same decreasing tendency, and it has to be noticed that their experiments were made mostly in the optimally and overdoped regions and in the presence of strong external fields.

4. Conclusions

In this work we have shown that the Boson-Fermion theory of superconductivity applied to a layered structure to represent $YBa_2Cu_3O_{6+x}$ cuprates produces excellent agreement with experimental data for their thermodynamic properties from zero to the critical temperature, such as the total isobaric specific heat as well as the entropy for doping values x ranging from 0.55 to 0.9. We show that the minimization of the electronic Helmholtz free energy coupled with the experimental critical temperature provides two optimum model parameters which are enough to reproduce the electronic specific heat constants $\alpha, \gamma_n(T_c)$ and the total specific heat constant for low temperatures β_l, as functions of doping.

The total isobaric specific heat *vs* temperature for all the doping values considered, coincides with the experimental data within a 5 % error range, where the lattice specific heat is included.

On the other hand, our curve for $\Delta C_p/T_c$ as a function of doping shows a decreasing tendency, contrary to what is experimentally observed, which could be an indirect confirmation that for temperatures near T_c there are other phenomena not considered in our model, such as the suppression of the spin susceptibility and oxygen disorder, which nevertheless do not affect the magnitude of $C_p(T)$.

The model gives inherently a direct relation between the layered structure of the cuprates and the mass anisotropy without the need to introduce external magnetic fields to measure it, which gives results of the same order of magnitude as experimental values.

It is worth mentioning that our model, in spite of the fact that it ignores particle interactions between composite bosons and unpaired electrons, nevertheless produces good results thereby suggesting that the effects of the layered structure are dominant.

Acknowledgements

References

1. G. Bednorz and K. A. Müller, Z. Phys. **B64**, 1175 (1986).

14   *P. Salas et al.*

2. J. Bardeen, L. N. Cooper and J. R. Schrieffer, Phys. Rev. **108**, 189 (1957).
3. A. Chubukov and P. J. Hirschfeld, Phys. Today **86**, 46 (2015).
4. D. C. Johnston, Adv. Phys. **59**, 803 (2010).
5. A. P. Drozdov, M. I. Eremets, I. A. Troyan, V. Ksenofontov and S. I. Shylin, Nature Letters **525**, 73 (2015).
6. J. E. Hirsh and F. Marsiglio, Physica **C511**, 45 (2015).
7. M. Sutherland, *et. al.*, Phys. Rev. **B67**, 174520 (2003).
8. S. E. Sebastian, N. Harrison, M. M. Altarawneh, C. H. Mielke, R. Liang, D. A. Bonn, W. N. Hardy and G. G. Lonzarich, PNAS **107**, 6175 (2010).
9. S. I. Schlachter, *et. al.*, Int. Jou. Mod. Phys. **B14**, 3673 (2000).
10. R. Liang, D. A. Bonn and W. N. Hardy, Phys. Rev. **B73**, 180505 (2006).
11. R. Friedberg and T. D. Lee, Phys. Letters A **138**, 423 (1989); R. Friedberg and T. D. Lee, Phys. Rev. **B40**, 6745 (1989).
12. R. Friedberg, T. D. Lee and H. C. Ren, Phys. Letters **A152**, 417 (1991).
13. M. Casas, N. J. Davidson, M. de Llano, T. A. Mamedov, A. Puente, R. M. Quick, A. Rigo, and M. A. Solís, Physica **A295**, 425 (2001).
14. A. Junod, A. Erb and Ch. Renner, Physica **C317**, 333 (1999).
15. D. M. Eagles, Phys. Rev. **186**, 456 (1969).
16. V. Tolmachev, Phys. Lett. **A266**, 400 (2000).
17. M. de Llano, F. J. Sevilla, S. Tapia, Int. Jou. of Mod. Phys. **B20**, 2931 (2006).
18. P. Salas, M. Fortes, M. de Llano, F. J. Sevilla, and M. A. Solís, J. of Low Temp. Phys. **159**, 540 (2010).
19. P. Salas, F. J. Sevilla, M. Fortes, M. de Llano, A. Camacho, and M. A. Solís, Phy. Rev. **A82**, 033632 (2010).
20. P. Salas, and M. A. Solís, J. of Low Temp. Phys. **175**, 427 (2014).
21. M. R. Norman, D. Pines and C. Kallin, Adv. Phys **54**, 715 (2005).
22. U. Tutsch, P. Schweiss, H. Wühl, B. Obst and Th. Wolf, Eur. Phys. Jou. **B41**, 471 (2004).
23. C. Meingast, A. Inaba, R. Heid, V. Pankoke, K-P Bohnen, W. Reichardt and T. Wolf., J. Phys. Soc. Jap. **78**, 074706 (2009).
24. J. L. Tallon and J. W. Loram, Physica **C349**, 53 (2001).
25. J. L. Tallon, F. Barber, J. G. Storey and J. W. Loram, Phys. Rev. **B87**, 140508 (2013).
26. P. Salas, M. Fortes, M. A. Solís and F. J. Sevilla, Physica **C524**, 37 (2016).
27. S. K. Adhikari, M. Casas, A. Puente, A. Rigo, M. Fortes, M. A. Solís, M. de Llano, A. A. Valladares and O. Rojo, Phys. Rev. **B62**, 8671 (2000).
28. Y. J. Uemura, Physica **B374**, 1 (2006).
29. Ch. Niedermayer, C. Bernhard, U. Binninger, H. Glückler, J. L. Tallon, E. J. Ansaldo and J. I. Budnick, Phys. Rev. Lett. **71**, 1764 (1993).
30. S. K. Adhikari, M. de Llano, F. J. Sevilla, M. A. Solís and J. J. Valencia, Physica **C453**, 37 (2007).
31. R. K. Pathria, *Statistical Mechanics*, 2nd Ed. (Pergamon, Oxford, 1996).
32. H. Alloul, T. Ohno and P. Mendels, Phys. Rev. Lett. **63**, 1700 (1989).
33. S. C. Riggs, O. Vafek, J. B. Kemper, J. B. Betts, A. Migliori, F. F. Balakirev, W. N. Hardy, R. Liang, D. A. Bonn and G. S. Boebinger, Nat. Phys. **7**, 332 (2011).
34. J. W. Loram, K. A. Mirza, J. R. Cooper, W. Y. Liang and J. M. Wade, Jou. of Sup. **7**, 243 (1994).
35. D. A. Wright, J. P. Emerson, B. F. Woodfield, J. E. Gordon, R. A. Fisher and N. E. Phillips, Phys. Rev. Lett. **82**, 1550 (1999).
36. K. A. Moler, D. J. Baar, J. S. Urbach, R. Liang, W. N. Hardy and A. Kapitulnik, Phys. Rev. Lett **73**, 2744 (1994).

37. K. A. Moler, D. L. Sisson, J. S. Urbach, M. R. Beasley, A. Kapitulnik, D. J. Baar, R. Liang and W. N. Hardy, Phys. Rev. **B55**, 3954 (1997).
38. R. A. Fisher, J. E. Gordon, S. F. Reklis, D. A. Wright, J. P. Emerson, B. F. Woodfield, E. M. McCarron III and N. E. Phillips, Physica **C252**, 237 (1995).
39. J. P. Emerson, D. A. Wright, B. F. Woodfield, J. E. Gordon, R. A. Fisher and N. E. Phillips, Phys. Rev. Lett. **82**, 1546 (1999).
40. A. Junod, B. Revaz, Y. Wang and A. Erb, Physica **B162**, 1401 (2000).
41. M. Chiao, R. W. Hill, C. Lupien, L. Taillefer, P. Lambert, R. Gagnon and P. Fournier, Phys. Rev. **B62**, 3554 (2000).
42. Y. Wang, B. Revaz, A. Erb and A. Junod, Phys. Rev. **B63**, 094508 (2001).
43. A. Junod, D. Eckert, T. Graf, G. Triscone and J. Muller, Physica **C162**, 1401 (1989).
44. B. Revaz, J.-Y. Genoud, A. Junod, K. Neumaier, A. Erb and E. Walker, Phys. Rev. Lett. **80**, 3364 (1998).
45. G. Blatter, V. B. Geshkenbein, and A. I. Larkin, Phys. Rev Lett. **68**, 875 (1992).
46. M. Roulin, A. Junod, and E. Walker, Physica **C296**, 137 (1998).